

Stability and multi-attractor dynamics of a toggle switch based on a two-stage model of stochastic gene expression

Michael Strasser

Institute for Bioinformatics and Systems Biology,
Helmholtz Zentrum München
German Research Center for Environmental Health, Germany

Fabian J. Theis

Institute for Bioinformatics and Systems Biology,
Helmholtz Zentrum München
German Research Center for Environmental Health, Germany

and

Institute for Mathematical Sciences,
Technische Universität München
Garching, Germany

Carsten Marr^{1 2}

Institute for Bioinformatics and Systems Biology,
Helmholtz Zentrum München
German Research Center for Environmental Health, Germany

February 19, 2022

¹Corresponding author. Address: Institute for Bioinformatics and Systems Biology, Helmholtz Zentrum München, Ingolstaedter Landstrasse 1, 85764 Neuherberg, Germany, Tel.: +49 (0)89 3187 3642, Fax: +49 (0)89 3187 3585, Email: carsten.marr@helmholtz-muenchen.de

²Present address: Centre for Systems Biology at Edinburgh, University of Edinburgh, Edinburgh EH9 3JD, UK

Abstract

A toggle switch consists of two genes that mutually repress each other. This regulatory motif is active during cell differentiation and is thought to act as a memory device, being able to choose and maintain cell fate decisions. Commonly, this switch has been modeled in a deterministic framework where transcription and translation are lumped together. In this description, bistability occurs for transcription factor cooperativity, while autoactivation leads to a tristable system with an additional undecided state.

In this contribution, we study the stability and dynamics of a two-stage gene expression switch within a probabilistic framework inspired by the properties of the Pu/Gata toggle switch in myeloid progenitor cells. We focus on low mRNA numbers, high protein abundance and monomeric transcription factor binding. Contrary to the expectation from a deterministic description, this switch shows complex multi-attractor dynamics without autoactivation and cooperativity. Most importantly, the four attractors of the system, which only emerge in a probabilistic two-stage description, can be identified with committed and primed states in cell differentiation. We first study the dynamics of the system and infer the mechanisms that move the system between attractors using both the quasi-potential and the probability flux of the system. Second, we show that the residence times of the system in one of the committed attractors are geometrically distributed. We derive an analytical expression for the parameter of the geometric distribution, therefore completely describing the statistics of the switching process and elucidate the influence of the system parameters on the residence time. Most importantly we find that the mean residence time increases linearly with the mean protein level. This scaling also holds for a one-stage scenario and for auto-activation. Finally, we study the implications of this distribution for the stability of a switch and discuss the influence of the stability on a specific cell differentiation mechanism. Our model explains lineage priming and proposes the need of either high protein numbers or long term modifications such as chromatin remodeling to achieve stable cell fate decisions. Notably we present a system with high protein abundance that nevertheless requires a probabilistic description to exhibit multistability, complex switching dynamics and lineage priming.

Key words: stochastic processes; stochastic simulation; multistability; cell differentiation; escape time; potential landscape

1 Introduction

During differentiation, a cell and its progeny cascade through a number of lineage decisions from stem cells over progenitor cells to mature functional cells. Many decisions are assumed to be binary and realized by a toggle switch, a simple cellular memory device. This network module consists of two genes, inhibiting each other via mutual promoter binding. In each differentiating cell, one gene will eventually win this biomolecular battle, inhibiting the other gene and subsequently activating its lineage-determining downstream targets. In hematopoiesis, the generation of blood cells, a series of gene switches has been found to determine the differentiation path of hematopoietic stem cells and to direct the ratio of mature blood cells (1, 2). The most prominent example in this context is the mutual inhibition of Gata-1 and Pu.1, two transcription factors responsible for the development of erythroid and myeloid blood cells from common myeloid progenitors (3–5).

Due to its importance in development, toggle switches are subject to both experimental and theoretical investigations (for a review, see (6)). Using a deterministic framework under the assumption of large molecule numbers, Cherry and Adler (7) discussed criteria for working switches. More specifically Roeder and Glauche (8), Huang et al. (9) and Chickarmane et al. (10) used a simple deterministic model of the toggle switch based on ordinary differential equations in order to describe the Pu.1–Gata-1 switch in hematopoiesis. A comprehensive overview and comparison of the different deterministic toggle switch models is provided by Duff et al. (11).

All these studies focus on the steady states of the switch and the parameter dependent bifurcations in a deterministic framework. However, protein variations of a differentiating cell influence the dynamics of the decision making process and lead to stochastic transitions between the two steady states. This randomness is induced by gene expression noise, which has been shown to be ubiquitous in biological systems due to low molecule numbers (12). Thus, the probabilistic frameworks developed in order to account for gene expression noise (see (13) for a review) have to be applied in order to understand fundamental aspects of toggle switch properties.

Probabilistic models of the toggle switch account for low copy numbers and intrinsic fluctuations. In (14), the dynamics of an exclusive switch, where two genes share the same promoter, is discussed within a probabilistic framework. A comparison of simple switch circuitries is given in Warren and Ten Wolde (15). Contrary to deterministic models, transitions between the two macroscopic regimes where one of the two genes dominates are possible due to the inherently noisy gene transcription (16, 17), even without cooperative binding of transcription factors (18). More recent contributions focused on analytic descriptions (19, 20), the switching time between macroscopic regimes for different regulatory realizations (16, 21, 22) or parameter regimes (17), boundaries for the switching time (23), or delay effects (24). Notably, all of these approaches are based on a one-stage model of gene expression, where DNA is directly processed into functional proteins. However, it has been shown that the characteristics of protein noise strongly depend on the underlying expression model (25, 26).

In this contribution, we abstract the regulatory details of the prominent myeloid Pu.1-Gata-1 mutual inhibition. Contrary to common belief, which advocates the lumping of the two stages of expression, we show that the inclusion of both mRNA and protein leads to an interesting change in system dynamics. The probabilistic two-stage description exhibits complex multi-attractor dynamics without autoactivation and cooperativity. Remarkably, a recent study reported low numbers of mRNAs in single murine blood cells: Warren et al. (27) found around 10 transcripts of the Pu.1 gene per cell in common myeloid progenitors. Based on these findings we study a probabilistic description of a toggle switch with low mRNA numbers, high protein abundance and in accordance with the known role of Pu.1, monomeric transcription factor binding. We deliberately choose the simplest toggle switch model and neglect autoactivation due to our ignorance of the logic of activation and inhibition at the promoter. However our results can easily be extended and are

discussed for the case of dimeric regulation and exclusive autoactivation.

2 Results

2.1 A toggle switch based on a two-stage model of gene expression

We describe the mutual inhibition of two genes, further on called A and B, using a two-stage model of gene expression (25, 26) with mutual inhibition being realized as DNA-protein binding (see Fig. 1). This kind of switch has been implemented in vivo by Gardner et al. (28). The model can be represented as a set of biochemical reactions for A and B, respectively, and a set of reaction rates α , β , etc.:



Reactions 1 and 2 correspond to mRNA transcription from an unbound promoter and mRNA degradation, respectively. Reactions 3 and 4 resemble protein translation and degradation. The last two reactions 5 and 6 describe the binding and unbinding of a protein to the antagonistic gene and thereby the transition from an active to an inactive promoter and vice versa. Bound DNA lacks the ability to be transcribed. We would like to emphasize that here τ^+ and τ^- are rates rather than times. Note that we assume monomeric transcription factor binding as the simplest of regulatory interaction (which has recently been shown to be able to induce bimodal gene expression (29)). Our system's topology is symmetric with regard to the two genes, and so are the two columns of reactions 1–6 upon the exchange of gene labels A and B.

This model of gene expression is a highly simplified abstraction of the complex processes in the cell. Condensing transcription into a single biochemical reaction does not account for the various steps required to transcribe a gene, e.g. the assembly of the transcription initiation complex, unwinding of DNA or transition of the polymerase to elongation phase. Postprocessing and transport mechanisms are also neglected. However, simplified models of gene expression have successfully been applied to experimental data, supporting the validity of these simplifications (9, 30, 31).

Most commonly one will study the properties of the system in a deterministic framework using ordinary differential equations (ODEs) that describe the time-evolution of species concentrations (7–10). The ODEs can directly be inferred from reactions 1–6 assuming mass action kinetics:

$$\frac{d}{dt}d_A = \tau_B^-(1 - d_A) - \tau_B^+d_An_B \quad \frac{d}{dt}d_B = \tau_A^-(1 - d_B) - \tau_A^+d_Bn_A \quad (7)$$

$$\frac{d}{dt}m_A = \alpha_Ad_A - \gamma_A m_A \quad \frac{d}{dt}m_B = \alpha_Bd_B - \gamma_B m_B \quad (8)$$

$$\begin{aligned} \frac{d}{dt}n_A &= \beta_A m_A - \delta_A n_A \\ &+ \tau_A^-(1 - d_B) - \tau_A^+d_Bn_A \end{aligned} \quad \begin{aligned} \frac{d}{dt}n_B &= \beta_B m_B - \delta_B n_B \\ &+ \tau_B^-(1 - d_A) - \tau_B^+d_An_B \end{aligned} \quad (9)$$

where d_* is the abundance of unbound DNA $_*$, m_* is the abundance of mRNA $_*$ and n_* is the abundance of Protein $_*$ for $* \in \{A, B\}$.

Bound DNA is expressed in terms of unbound DNA due to mass conservation. Solving Eq. 7, 8 and 9 at steady state by setting all time derivatives to zero yields two solutions, one being biologically irrelevant due to its negative species abundances. Given non-negative initial conditions the system will always converge towards the positive steady state solution (32), given by (see Supporting Material for details)

$$m_A^{(ss)} = m_B^{(ss)} = -\frac{\delta\tau^-}{2\beta\tau^+} (1 - \eta) \quad (10)$$

$$n_A^{(ss)} = n_B^{(ss)} = -\frac{\tau^-}{2\tau^+} (1 - \eta) \quad (11)$$

$$d_A^{(ss)} = d_B^{(ss)} = \frac{2}{1 + \eta} \quad (12)$$

with $\eta = \sqrt{\frac{4\alpha\beta\tau^+}{\gamma\delta\tau^-} + 1}$. All parameters are positive and for simplicity assumed to be symmetric for players A and B ($\alpha = \alpha_A = \alpha_B, \dots$).

We now assess the stability of the positive solution Eq. 10 - 12 using standard linear stability analysis. To reduce the complexity of our system for the stability analysis, we apply a quasi steady state approximation to the DNA binding/dissociation process ($\dot{d}_A = \dot{d}_B = 0$), reducing the dimensionality of our system to four equations. We evaluate the corresponding Jacobian at the single positive solution and use the Hurwitz criterion to verify that all its eigenvalues have negative real part. We conclude that the system has one stable positive fixed point but we cannot analytically exclude the existence of limit cycles. However, inspection of the system's phase portrait (see Fig. S4 in the Supporting Material) indicates that no limit cycles exist. Summarizing, we showed that the deterministic model has only one steady state solution and is thus monostable.

However, since the deterministic approach is only valid in the limit of large numbers, small molecule numbers of DNA, mRNA, and possibly proteins advocate a discrete probabilistic description of the toggle switch. We define the state of the system at time t as a vector $x(t)$, where $x_i(t) \in \mathbb{N}_0$ is the abundance of species i at time t . Note that the state space is discrete as opposed to the deterministic model. To emphasize this difference we use the uppercase notation $D_A, D_B, M_A, M_B, N_A, N_B$ for the number of molecules of the respective species. We can describe how the probability $\mathcal{P}(x, t)$ of being in a certain state x changes over time by using the master equation of the system (33)

$$\dot{\mathcal{P}}(x, t) = \sum_{x'} [w_{xx'}\mathcal{P}(x', t) - w_{x'x}\mathcal{P}(x, t)] .$$

The first term considers transitions from states x' with rate $w_{xx'}$ to state x , while the second term accounts for transitions from x to all other possible states x' with transition rates $w_{x'x}$. The transition rates, also called propensities (34) are determined by the reaction rates and the number of reagents of the corresponding reactions (see Supporting Material 2 for an explicit form of the master equation of the system).

Even though the master equation describes the dynamics of the system more accurately than ODEs (most obviously for low particle numbers) it is still an approximation of cellular dynamics as it assumes spatial homogeneity inside a cell and does not account for time delays. Still, the protein distribution predicted by the master equation of a two-stage expression model was indeed observed experimentally (35), supporting the stochastic two-stage model.

Since the master equation for the switch is analytically solvable only for a number of approximations (see e.g. (36)) and not integrable for large molecule abundances, we simulate the system trajectories using Gillespie’s algorithm (37). Each trajectory follows the master equation, and the set of infinite trajectories constitutes the distribution that solves the master equation. To obtain appropriate parameters values for stochastic simulation, we delineate upper bounds for synthesis parameters from biophysical arguments and adapt degradation parameters to fit desired molecular levels. Table S1 in the Supporting Materials lists all used parameter values. Additionally, the analysis below has been conducted for a second, differently motivated, parameter set (see Fig. S3 in Supporting Material) and yields qualitatively identical results.

2.2 Dynamics and quasi-potential

In this section we discuss the main features of the switch dynamics. Contrary to the deterministic model, time courses of the stochastic toggle switch model show multistable behavior (Fig. 2A). Given the parameters in Table S1 our toggle switch can adopt different attractors: The two attractors where one player dominates the other (called S_A and S_B depending on which player dominates) are clearly visible in Fig. 2A. A careful inspection of the timecourse and the probability distribution in Fig. 2A shows that there also exist two intermediate attractors where protein numbers are similar ($N_A - N_B \approx 0$). These attractors are called S_A^* and S_B^* from now on. In the timecourses of the system (Fig. 2A) one observes that the system frequently switches between the dominating and the intermediate attractors.

To get a deeper understanding of the complex dynamics of the system the notion of a quasi-potential can be used. The quasi-potential U of the system is calculated through the relation $U(x) = -\log \mathcal{P}^{(ss)}(x)$, where $\mathcal{P}^{(ss)}(x)$ is the steady state distribution of the system. The number of dimensions of the state space where the quasi-potential is defined equals the number of species in the system. Here the probability $\mathcal{P}^{(ss)}(x)$ of a state x in steady state is estimated from 15000 stochastic simulation runs obtained by the Stochkit software toolkit (38). In Fig. 2B the projection of the quasi-potential on the $N_A - N_B$, $M_A - M_B$ plane is shown. The four attractors S_A , S_B , S_A^* and S_B^* can be seen clearly in the quasi-potential of the system. The two attractors S_A and S_B appear as basins at the lower left and upper right corner of Fig. 2 whereas the intermediate attractors S_A^* and S_B^* are located at the center and are not well separated. The dominating attractors can easily be distinguished from the intermediate attractors via parameter dependent thresholds χ_A, χ_B in the protein dimension (see Supporting Material 4).

Importantly, one has to keep in mind that the system considered is out of equilibrium and that the dynamics of a non-equilibrium system are not entirely determined by the gradient of the quasi-potential but by an additional curl flux stemming from the non-integrability of the system (39). As a consequence barrier heights in the quasi-potential do not necessarily correlate with the probability of crossing the barrier.

To understand the dynamics of the switch in more detail we therefore consider for each state x in the

state space the outflux $F(x)$ acting on the the system at this point (16). We calculate the outflux as:

$$F(x) = \mathcal{P}^{(ss)}(x) \sum_y \mathcal{P}(y|x)(y - x),$$

where the probability $\mathcal{P}(y|x)$ of state y succeeding state x and the probability $\mathcal{P}^{(ss)}(x)$ are calculated from stochastic simulations. Note that the outflux is different from the concept of field lines used in phase portraits of ordinary differential equations. The outflux $F(x)$ is plotted as small arrows in Fig. 2 (vectors are normalized and circles correspond the origin of the vectors) for all states x with $\mathcal{P}^{(ss)}(x) > 2.5 \cdot 10^{-7}$. This indicates where the system will move from the current state on average. Due to this outflux the system enters and leaves the attractors S_A and S_B through different paths. This phenomenon has been described in (40) and linked to the emergence of time directionality in non-equilibrium systems. In order to move from high (S_A or S_B) to low (S_0) protein numbers, at first the corresponding mRNA number has to drop. On the contrary, moving from low to high protein numbers requires the rise of mRNA numbers first.

A different view on the system's dynamics is provided by the quasi-potential landscape and outflux in the $N_A^{\text{total}}, N_B^{\text{total}}$ plane (Fig. 3), where $N_A^{\text{total}} = (1 - D_B) + N_A$ is the total number of Protein_A in the system, bound to DNA (first term) or free (second term). Choosing N_A^{total} and N_B^{total} as projected dimensions shows four distinct basins in the quasi-potential landscape. Two basins correspond to the attractors S_A and S_B . These are characterized by high amounts of the dominating protein and zero proteins of the repressed species. The attractors S_A^* and S_B^* are now clearly separated. In these two basins a single protein of one species is present and only a moderate protein number of the other species. In the following we show why these basins emerge and how the system moves between the attractors.

We explain the dynamics of the system with a typical trajectory of the system: Let us start with the trajectory in the attractor S_A (lower right) where Protein_A dominates Protein_B. Due to stochastic fluctuations in the promoter status, eventually a burst of proteins of B will occur and inhibit the promoter of A, whose protein numbers will drop (Fig. 3, trajectory I). While the formerly dominating Protein_A's are degraded, also the newly created Protein_B quickly decreases in numbers and only one bound Protein_B is saved from degradation. This drives the system towards the origin in the quasi-potential of Fig. 3. However, a single Protein_B cannot completely suppress the promoter of DNA_A, leading to a small but constant synthesis of Protein_A. The system settles into an intermediate state (S_A^*) defined by the presence of one Protein_B and an intermediate amount of Protein_A originating from the leaky inhibition of DNA_A and bursting. In order to leave this basin the system has two options: Either the single Protein_B is degraded when it momentarily is not bound to the promoter. Consequently the levels of Protein_A rise again and the system reaches S_A . The system is moved to the lower border of the quasi-potential where a strong outflux pushes it towards S_A (Fig. 3, trajectory II). Alternatively, a burst of Protein_B displaces the system from S_A^* into regions where the vector field points strongly towards the diagonal $N_A^{\text{total}} = N_B^{\text{total}}$ (Fig. 3, trajectory III). However this burst is typically not strong enough to move the system onto the diagonal and it will fall back into the basin S_A^* . In order to enable a change from S_A^* to S_B^* the system has to reach the diagonal. This is accomplished if, while the system is moving towards the diagonal after the burst, additional bursts of Protein_B move it onto the diagonal (Fig. 3, trajectory IV). Once the system has hit the diagonal both protein levels will drop to very low numbers since non of the players has any significant advantage. Here by chance the system will move to any side of the diagonal and either towards S_A^* or S_B^* (Fig. 3, trajectories V, VI).

We find that leaving S_A^* towards S_A (Fig. 3, trajectory II) is much more probable than hitting the diagonal from S_A^* (Fig. 3, trajectory IV), which would provide the chance of switching. This is obvious from the mechanism described above: Even though the events triggering the two alternatives (degradation of Protein_B and an initial burst of Protein_B) have similar probabilities, the diagonal crossing requires additional events and is therefore much less probable. This cannot be deduced from the quasi-potential landscape alone: From

Fig. 3 it can visually be inferred that the barrier separating S_A and S_A^* is higher than the barrier separating S_A^* and S_B^* . This wrongly suggests that moving between S_A^* and S_B^* occurs more frequently than moving between S_A and S_A^* .

Comparing the system dynamics of our switch with other descriptions we find that (i) deterministic one-stage and two-stage models show no bistability while (ii) a probabilistic one-stage model exhibits tristability with only one intermediate attractor (see Fig. S2 in the Supporting Material and (29)). We speculate that translational bursting destabilizes the intermediate attractor of the one-stage model, where none of the two players can overwhelm the other. Bursting provides an easy mechanism to escape this deadlock situation: It gives the player whichever bursts first a huge advantage over the other, giving rise not only to one protein (as in the one-stage model) but several proteins. As a result, the two-stage system is always quickly pushed away from the diagonal and stabilizes in the attractors S_A^* or S_B^* . Thus, only the combination of a probabilistic description with a two-stage model of gene expression leads to the complex multi-attractor dynamics described above.

2.3 Residence times

Genetic toggle switches are thought to be involved in the differentiation process of cells. A common idea is that different cell fates correspond to the different attractors of the system (41). Therefore it is of interest how long the system will stay in one of these attractors. In this contribution, we focus on the time the system will stay in the attractors S_A or S_B . We assume that only in these two attractors the concentration of either player is sufficiently high to carry out a downstream biological function which resembles the switch's decision.

In previous contributions, such quantities have been calculated or determined by stochastic simulation for simpler switch models and were called spontaneous switching time (23), switch lifetime (15), mean first-passage time (14), or switching time (22). Since the switch may flip from a dominating to an intermediate attractor, we choose residence time as the appropriate term for the quantity calculated below. In the following, we derive an analytical approximation for the time the switch stays in a dominating attractor, S_A or S_B , called the residence time t_s . A simulation study for S_A^*/S_B^* suggests qualitatively similar behavior (see Fig. S5 in the Supporting Material).

Let us assume that the system is in attractor S_A . Hence, the promoter of DNA_B is bound by Protein_A while the promoter of DNA_A is unbound. We assume that the protein levels in this attractor can be described with the simple two-stage model (25), resulting in a mean Protein_A level of $\bar{N}_A = (\alpha_A \beta_A) / (\gamma_A \delta_A)$. Consequently, the protein level of Protein_B is $N_B = 0$ as it is inhibited by the high levels of Protein_A . In order to leave S_A it is crucial that one Protein_B is synthesized, which then can bind the promoter of DNA_A and shut down the synthesis of Protein_A , ultimately driving the system out of S_A and into S_A^* . This trajectory (called trajectory I in Fig. 3) involves the following events: (i) unbinding of Protein_A from DNA_B , (ii) synthesis of Protein_B during the unbound phase, and (iii) binding of Protein_B to the promoter of DNA_A before Protein_B is degraded.

First we describe the unbinding of Protein_A from DNA_B . While the system is in S_A , Protein_A dissociates various times, leaving the promoter of DNA_B unbound. The average time the promoter remains unbound, t_u , is equal to the average time until a binding reaction occurs, which is

$$t_u = \frac{1}{\tau_A^+ \cdot \bar{N}_A}.$$

The time the promoter stays unbound is a random variable itself, but for simplicity we approximate it with its mean value. Note that t_u depends, somewhat counterintuitively, on τ^+ and not on τ^- , with $\tau_A^+ \bar{N}_A$ being the propensity for a binding reaction. Again we emphasize that τ^+ and τ^- are rates (rather than times).

To ultimately synthesize a Protein_B, at least one mRNA_B has to be transcribed during t_u and translated before degradation. The probability of k transcription reactions to happen during t_u is

$$P_{\text{Poisson}}(K = k) = \frac{(\alpha_B \cdot t_u)^k}{k!} \cdot \exp(-\alpha_B \cdot t_u),$$

as the number of transcription reactions K during t_u is Poisson-distributed with mean $\alpha_B \cdot t_u$. Thus, the probability of at least one transcription during the unbound phase is

$$q_s = 1 - P(K = 0) = 1 - \exp\left(-\frac{\alpha_B}{\tau_A^+ \cdot \bar{N}_A}\right).$$

The probability of translation during an average mRNA lifetime $1/\gamma_B$ is accordingly $q_t = 1 - \exp(-\beta_B/\gamma_B)$. Finally the probability for a binding reaction during average protein lifetime $1/\delta_B$ is $q_b = 1 - \exp(-\tau_B^+/\delta_B)$.

However, not only one but several unbound phases may occur before Protein_B is successfully synthesized. The number L of unbound phases until and including successful synthesis follows a geometric distribution, $P(L = l) = (1 - q)^{l-1}q$ with parameter $q = q_s \cdot q_t \cdot q_b$. The average number of unbound phases during a time interval Δt is $\tau_A^- \cdot \Delta t$. Thus, we can convert the random variable L into $T = L/\tau_A^-$ via a linear transformation of a random variable, giving the actual time until successful synthesis of Protein_B. Notably, the derivation of the distribution for residence times goes beyond previous mean-field approximations. Using the properties of the geometric distribution for the random variable T , we end up with the mean and the variance of the residence time:

$$t_s = \frac{1}{\tau_A^- \cdot q_s q_t q_b} \quad \text{and} \quad \sigma_{t_s}^2 = \frac{1}{(\tau_A^-)^2} \cdot \frac{1 - q_s q_t q_b}{(q_s q_t q_b)^2}. \quad (13)$$

An important approximation for the residence time can be derived under the assumption of rapid translation and slow mRNA degradation, $\beta \gg \gamma$, leading to $q_t \approx 1$. This implies that it is quite certain that an mRNA will be translated at least once before degradation. In the regime of rapid transcription factor binding ($\tau^+ \gg \delta, \alpha$) the probability for a binding reaction is close to one, $q_b \approx 1$, while the probability for at least one transcription can be approximated with $q_s \approx \alpha_B/(\tau_A^+ \bar{N}_A)$. Taken together, this leads to a linear dependence of the residence time on the protein number,

$$t_s \approx (\tau_A^+/\tau_A^-) \cdot (\bar{N}_A/\alpha_B). \quad (14)$$

We want to compare our analytical approximation with the residence time derived from simulations. To that end, we have to infer the dominating attractors from the simulated time courses. Recall that we can identify the dominating attractors via thresholds χ_A, χ_B at protein levels. The residence time of attractor S_A (S_B) is estimated as the consecutive time in a trajectory where $N_A > \chi_A$ ($N_B > \chi_B$). We compare the analytically derived geometric distribution for the residence times (see Eq. 13) with numerical results by simulating the switch with a given parameter set and estimating the residence times from 10000 stochastic simulations. Fig. 4A shows excellent agreement between the geometric distributed residence time and the simulations for a protein degradation rate of $\delta = 8 \cdot 10^{-4} \text{s}^{-1}$. This legitimates the approximations and assumptions made above for the parameter regime of rapid transcription factor binding. From the analysis of the mean residence time for different protein half-lives, we find again a good agreement between the simulation and the approximation (see Fig. 4B). Moreover, the slope of the log-log curve of the simulation is 1 – confirming a linear dependence of the residence time from the mean protein level.

With the result from Eq. 13 we can compare the mean residence time of different switch models. First we consider a gene expression model where transcription and translation are condensed into a single protein

synthesis reaction. In analogy to the two-stage model of gene expression (26), this can be called a one-stage model of gene expression. To achieve the same amount of proteins at similar degradation rates, the synthesis rate in the one-stage model needs to be larger compared to the transcription and translation rates in the two-stage model. The probability q_t which accounts for translation during mRNA lifetime can be set to 1, since there is no mRNA stage and proteins are produced immediately. The binding probability q_b remains unchanged. However, because of the increased synthesis rate, the probability q_s of synthesis during the unbound phase will be larger than in the two-stage model. Therefore, the mean residence time will be decreased in the one-stage model as compared to the two-stage model, leading to more frequent attractor changes. This finding is in accordance with the previously reported stabilizing effect of bursts in an exclusive switch (16).

A second modification of the switch includes not only mutual inhibition but also autoactivation of both genes. If the promoter of the gene is unbound it will be transcribed with a small basal rate κ . If the promoter is bound by its own protein product the gene will be transcribed with full rate $\alpha \gg \kappa$. Repressor bound promoters are inactive. For simplicity we assume that either activators or repressors are bound but not both at the same time. Note that in this case also the deterministic ODE model is bistable (42). Considering the mean residence time in a two-stage switch with autoactivation, we find that the probability q_s of mRNA synthesis during the unbound phase is smaller than in the ordinary two-stage model. Since no activator is present in this attractor, mRNA has to be transcribed with the small basal rate κ , making the transcription more improbable. The probability q_t for translation remains unchanged. However, the probability q_b of protein binding to the antagonistic promoter is also decreased since this promoter is occupied by the abundant activator most of the time. Therefore, repressor binding to this promoter requires an additional dissociation reaction of the activator during repressor lifetime. As both q_s and q_b are decreased the mean residence time in switch models with autoactivation will be strongly increased compared to the ordinary two-stage model.

Summarizing, we find that the residence time is (i) geometrically distributed, (ii) the mean of the distribution grows linearly with the number of proteins for slow mRNA degradation, and (iii) both the intermediate step of mRNA production and the autoactivation of transcription factors increase the residence time.

3 Discussion

3.1 Lineage priming

We now discuss the implications of our findings in the context of cell differentiation driven by the toggle switch. In previous studies (8, 9, 40), attractors where either one or the other player is dominating, thereby repressing the antagonist (S_A , S_B) corresponded to committed cells. We also find analogs for the intermediate states S_A^* and S_B^* . In these attractors the system has a strong preference towards one specific dominating attractor, but is not fully committed yet. A similar behavior is known as lineage priming in stem cell biology (43). Two different studies (44, 45) showed that a population of stem and progenitor cells, respectively, can be divided into subpopulations that mainly give rise to only one of two possible cell types. In our simple model this would correspond to stem cells that reside either in S_A^* or S_B^* . These stem cells can still give rise to both cell fates but have a strong tendency towards one of them.

Remarkably only a two-stage probabilistic model of the toggle switch shows dynamics reminiscent of lineage priming. Although a progenitor state exists in one-stage models of the toggle switch, cells in this state will move to either the one or the other committed state with equal probability.

3.2 Residence time

We find that the residence time in S_A and S_B , a key property of the system, is geometrically distributed. Previous contributions (22, 23, 46) focused only on the mean residence time and did not consider its underlying distribution. What does a geometric distribution for the residence time imply for the differentiation process dependent on the state of a genetic switch? To discuss this question, let us first reason on how a differentiation decision could be established with the toggle switch lined out in the previous sections.

We discriminate two scenarios for the differentiation of a cell: In the first scenario, the state of the switch completely determines the cell fate. Starting in the progenitor attractors S_A^* or S_B^* , after a certain amount of time, the switch will move to a committed attractor. We assume that the high numbers of proteins of the dominating player will trigger the differentiation program of the associated lineage and establish the mature cell type. However due to stochasticity, the switch will drop out of the committed attractors and the cell will not only lose the current lineage decision, but possibly even switch to the opposing cell fate. In order to establish stable lineages in this scenario, the cell has to assure that the residence time of the switch is much longer than all relevant biological processes of the cell, especially cell lifetime. This guarantees that the cell will keep a lineage decision once it has obtained one. Yet the geometric distribution of the residence time imposes difficulties in this scenario: Even if the mean residence time is high, short residence times will always be more probable than longer residence times. The toggle switch could either be stabilized with the aforementioned autoactivation of the players, or with very high protein numbers so that the geometric distribution flattens and transforms to an almost uniform distribution. Both means would assure that only a very small percentage of a population of cells forgets its lineage decision during lifetime.

In the second scenario we assume that the cell gets locked in one fate by changing the shape of the underlying potential so that further transitions between attractors become less possible. Such a change of the potential could for example be facilitated by chromatin changes, as proposed by Akashi et al. (47). In the following, we assume that only if one state dominates the other for a long enough fixation time t_d , downstream genes necessary for the decision process are activated (e.g. leading to chromatin remodeling), and the cell differentiates. Such a time depending property could be implemented with low-pass filters (see (48) for an example in hematopoietic stem cells) and would allow for an integration of external signals (see (49) for the instructive power of hematopoietic cytokines). In this scenario, the residence time determines when differentiation will occur: The switch will constantly move into and out of the dominating attractors, until the residence time is finally long enough so that the dominating player can activate the downstream differentiation machinery. Ignoring the time the system spends in the intermediate attractors and just summing up the residence times in S_A and S_B until a long enough residence time for differentiation occurs, we find that this time follows a geometric-like distribution (see Supporting Material 5). Under this differentiation mechanism, most cells will differentiate very fast and only few cells will need longer. Experiments that measure the time for single cells needed to go from the primed to the committed state (as an extension to the 2-day threshold reported by Heyworth et al. (50) for GM-CTC cells) in order to support or reject these hypotheses remain to be done.

3.3 Comparison to previous models

Finally we discuss how our findings relate to previous studies on the toggle switch. We found that the mean of the residence time distribution scales linearly with the number of proteins in the system. The more proteins are present, the longer the average residence time in S_A or S_B . However, shorter residence times are still most probable due to the geometric distribution. This holds for the one-stage, the two-stage, and the auto-activating scenario.

This linear scaling differs from the exponential (23) or near exponential (46) scaling described previously

in the one-stage scenario. In contrast to our model, the model of Warren and ten Wolde (46) considers dimerization of the transcription factors, motivated by the fact that cooperative binding is necessary to achieve bistability in a deterministic framework (10). We showed that, as soon as stochastic fluctuations are introduced, a system with multiple attractors is achieved that can act as a proper switch with additional states of low co-expression. Including dimerization as a prerequisite for inhibition in a one-stage model will strongly increase the stability of the attractors $S_{A/B}$ (46). This is consistent with our findings: Instead of requiring translation of one protein of the suppressed species, we now require this rare event to happen twice during a short time frame, which is much less probable. However, the inclusion of dimerization will have less effect on the two-stage switch: Since proteins are typically synthesized in bursts (in our model the average burst size is $\beta/\gamma = 10$) and dimerization is a fast process (46), as soon as one burst occurs almost certainly a dimer is formed and can inhibit the currently dominating player. Therefore the probability of leaving the attractors $S_{A/B}$ is similar to a non-dimeric inhibition.

Contrary to our results, Warren and ten Wolde (46) report that introduction of mRNAs reduces the stability of the switch. This discrepancy can be understood in the light of dimerization. In their one-stage model dimerization is a key ingredient of stability, which is lost when introducing translational bursts ("shot noise"). As we considered monomeric transcription factor binding, stability does not rely on dimerization. Therefore mRNAs increase the stability of the system, because they introduce additional conditions required for switching.

Due to these differences in the model it is hard to resolve the discrepancy between our linear and the exponential scaling of residence time found by Bialek (23) and Warren and ten Wolde (46). However we want to emphasize that the theoretical results shown in (46) only consider protein numbers up to 30. In this region our simulation results show slight deviations from the analytical linear dependence (Fig. 4). At such low protein numbers the system does not only leave the dominating attractor according to the mechanism described in our results. It is also likely that just due to fluctuations in the gene expression (not fluctuations in the promoter) the dominating attractor is left. This mechanism operates only at very small protein numbers and its probability rapidly decreases with rising protein numbers. Therefore our results do not contradict the findings of Warren and ten Wolde (46), but consider a different parameter regime with higher protein numbers. Interestingly, the noise-driven attractor changes are also described by Kashiwagi et al. (51) where the authors link this mechanism to the selection of a favorable, less noisy attractor in *E. Coli* populations.

In another contribution, Morelli et al. (52) use the forward flux sampling algorithm to assess the stability of a one-stage genetic toggle switch with dimeric transcription factor binding. They find a similar mechanism of attractor flipping which is based on the synthesis of the suppressed species due to promoter fluctuations. Using the forward flux sampling, they obtain estimates of the switching rate (the inverse of the mean residence time) for different amounts of fluctuations in DNA-protein interaction and dimerization. Morelli et al. (52) modulate the size of fluctuations at the promoter by varying the ratio of binding rate and synthesis rate, the adiabaticity parameter $\omega = \tau^+/\alpha$ (τ^- is adjusted to keep τ^+/τ^- constant). Small ω leads to strong fluctuations, whereas large ω reduces fluctuations. They find that increasing ω decreases the average switching rate and therefore stabilizes the switch. This dependency vanishes for $\omega > 5$, where the average switching rate remains constant. The latter is in accordance with our results in Eq. 14, where the mean residence time depends only on the ratio of τ^+ and τ^- , not on the absolute values and is therefore independent of ω . The dependency of the average switching rate for $\omega < 5$ is not predicted by Eq. 13 and 14. It is also not visible in the stochastic simulations, where mean residence times of systems with $\omega = 1$ and $\omega = 20$ coincide (Fig. 4). The results of Morelli et al. (52) were simulated for an average number of proteins $\bar{N}_A = \bar{N}_B = 27$. As mentioned above, in regions of very small protein numbers the system might leave the dominating attractor by a mechanism not captured by Eq. 13 and 14, probably causing the difference of the

results of Morelli et al. (52) and our results for small ω .

Acknowledgments

We thank Jan Krumsiek, Robert Schlicht, Timm Schroeder and Peter Swain for stimulating discussions and Christiane Dargatz and Dominik Wittmann for careful reading and thoughtful feedback on drafts of this manuscript. Thanks to Sabine Hug and Daniel Schmidl for their help concerning the stability analysis. Moreover we acknowledge the comments of the unknown reviewers, who improved the quality of the manuscript.

This work was supported by the Helmholtz Alliance on Systems Biology (project 'CoReNe'), the European Research Council (starting grant 'LatentCauses'), and the German Science Foundation DFG (postdoc fellowship for C.M. and SPP 1356 'Pluripotency and Cellular Reprogramming').

References

1. Orkin, S. H., and L. I. Zon, 2008. SnapShot: hematopoiesis. *Cell* 132:712.
2. Krumsiek, J., C. Marr, T. Schroeder, and F. J. Theis, 2011. Hierarchical Differentiation of Myeloid Progenitors Is Encoded in the Transcription Factor Network. *PLoS ONE* 6:e22649.
3. Zhang, P., G. Behre, J. Pan, A. Iwama, N. Wara-Aswapati, H. S. Radomska, P. E. Auron, D. G. Tenen, and Z. Sun, 1999. Negative cross-talk between hematopoietic regulators: GATA proteins repress PU.1. *Proc Natl Acad Sci USA* 96:8705–8710.
4. Arinobu, Y., S.-i. Mizuno, Y. Chong, H. Shigematsu, T. Iino, H. Iwasaki, T. Graf, R. Mayfield, S. Chan, P. Kastner, and K. Akashi, 2007. Reciprocal activation of GATA-1 and PU.1 marks initial specification of hematopoietic stem cells into myeloerythroid and myelolymphoid lineages. *Cell Stem Cell* 1:416–427.
5. Burda, P., P. Laslo, and T. Stopka, 2010. The role of PU.1 and GATA-1 transcription factors during normal and leukemogenic hematopoiesis. *Leukemia* 24:1249–1257.
6. Macarthur, B. D., A. Ma'ayan, and I. R. Lemischka, 2009. Systems biology of stem cell fate and cellular reprogramming. *Nat Rev Mol Cell Biol* 10:672–81.
7. Cherry, J. L., and F. R. Adler, 2000. How to make a biological switch. *J Theor Biol* 203:117–133.
8. Roeder, I., and I. Glauche, 2006. Towards an understanding of lineage specification in hematopoietic stem cells: a mathematical model for the interaction of transcription factors GATA-1 and PU.1. *J Theor Biol* 241:852–865.
9. Huang, S., Y.-P. Guo, G. May, and T. Enver, 2007. Bifurcation dynamics in lineage-commitment in bipotent progenitor cells. *Dev Biol* 305:695–713.
10. Chickarmane, V., T. Enver, and C. Peterson, 2009. Computational Modeling of the Hematopoietic Erythroid-Myeloid Switch Reveals Insights into Cooperativity, Priming, and Irreversibility. *PLoS Comput Biol* 5:e1000268.
11. Duff, C., K. Smith-Miles, L. Lopes, and T. Tian, 2011. Mathematical modelling of stem cell differentiation: the PU.1-GATA-1 interaction. *Journal of mathematical biology* .

12. Eldar, A., and M. B. Elowitz, 2010. Functional roles for noise in genetic circuits. *Nature* 467:167–173.
13. Paulsson, J., 2005. Models of stochastic gene expression. *Physics of Life Reviews* 2:157–175.
14. Kepler, T. B., and T. C. Elston, 2001. Stochasticity in transcriptional regulation: origins, consequences, and mathematical representations. *Biophys J* 81:3116–36.
15. Warren, P., and P. Ten Wolde, 2004. Enhancement of the stability of genetic switches by overlapping upstream regulatory domains. *Phys Rev Lett* 92:128101.
16. Schultz, D., A. M. Walczak, J. N. Onuchic, and P. G. Wolynes, 2008. Extinction and resurrection in gene networks. *Proceedings of the National Academy of Sciences of the United States of America* 105:19165–70.
17. Walczak, A. M., J. N. Onuchic, and P. G. Wolynes, 2005. Absolute rate theories of epigenetic stability. *Proceedings of the National Academy of Sciences of the United States of America* 102:18926–31.
18. Lipshtat, A., A. Loinger, N. Q. Balaban, and O. Biham, 2006. Genetic toggle switch without cooperative binding. *Phys Rev Lett* 96:188101.
19. Walczak, A., M. Sasai, and P. Wolynes, 2005. Self-Consistent Proteomic Field Theory of Stochastic Gene Switches. *Biophys J* 88:828–850.
20. Schultz, D., J. N. Onuchic, and P. G. Wolynes, 2007. Understanding stochastic simulations of the smallest genetic networks. *J Chem Phys* 126:245102.
21. Loinger, A., A. Lipshtat, N. Q. Balaban, and O. Biham, 2007. Stochastic simulations of genetic switch systems. *Phys Rev E Stat Nonlin Soft Matter Phys* 75:021904.
22. Barzel, B., and O. Biham, 2008. Calculation of switching times in the genetic toggle switch and other bistable systems. *Phys Rev E Stat Nonlin Soft Matter Phys* 78:041919.
23. Bialek, W., 2001. Stability and noise in biochemical switches. *In Advances in neural information processing systems* 13. The MIT Press, 103.
24. Zhu, R., A. S. Ribeiro, D. Salahub, and S. A. Kauffman, 2007. Studying genetic regulatory networks at the molecular level: delayed reaction stochastic models. *J Theor Biol* 246:725–45.
25. Thattai, M., and A. van Oudenaarden, 2001. Intrinsic noise in gene regulatory networks. *Proc Natl Acad Sci USA* 98:8614–9.
26. Shahrezaei, V., and P. S. Swain, 2008. Analytical distributions for stochastic gene expression. *Proc Natl Acad Sci USA* 105:17256–61.
27. Warren, L., D. Bryder, I. L. Weissman, and S. R. Quake, 2006. Transcription factor profiling in individual hematopoietic progenitors by digital RT-PCR. *Proc Natl Acad Sci USA* 103:17807–12.
28. Gardner, T., C. Cantor, and J. Collins, 2000. Construction of a genetic toggle switch in *Escherichia coli*. *Nature* 403:339–42.
29. Lipshtat, A., A. Loinger, N. Balaban, and O. Biham, 2006. Genetic Toggle Switch without Cooperative Binding. *Physical Review Letters* 96:1–4.

30. Harper, C. V., B. Finkenstädt, D. J. Woodcock, S. Friedrichsen, S. Semprini, L. Ashall, D. G. Spiller, J. J. Mullins, D. a. Rand, J. R. E. Davis, and M. R. H. White, 2011. Dynamic analysis of stochastic transcription cycles. *PLoS biology* 9:e1000607.
31. Raj, A., C. S. Peskin, D. Tranchina, D. Y. Vargas, and S. Tyagi, 2006. Stochastic mRNA synthesis in mammalian cells. *PLoS biology* 4:e309.
32. Mueller Herold, U., 1975. General mass-action kinetics. Positiveness of concentrations as structural property of Horn's equation. *Chemical Physics Letters* 33:467–470.
33. Van Kampen, N. G., 1992. Stochastic Processes in Physics and Chemistry. North-Holland, Amsterdam.
34. Gillespie, D. T., 2007. Stochastic simulation of chemical kinetics. *Annu Rev Phys Chem* 58:35–55.
35. Taniguchi, Y., P. J. Choi, G.-W. Li, H. Chen, M. Babu, J. Hearn, A. Emili, and X. S. Xie, 2010. Quantifying E. coli proteome and transcriptome with single-molecule sensitivity in single cells. *Science (New York, N.Y.)* 329:533–8.
36. Walczak, A., A. Mugler, and C. Wiggins, 2010. Analytic methods for modeling stochastic regulatory networks. *Arxiv preprint arXiv:1005.2648*.
37. Gillespie, D., et al., 1977. Exact stochastic simulation of coupled chemical reactions. *J. Phys. Chem* 81:2340–2361.
38. Li, H., Y. Cao, L. R. Petzold, and D. T. Gillespie, 2008. Algorithms and Software for Stochastic Simulation of Biochemical Reacting Systems. *Biotechnology Progress* 24:56–61.
39. Wang, J., L. Xu, and E. Wang, 2008. Potential landscape and flux framework of nonequilibrium networks: robustness, dissipation, and coherence of biochemical oscillations. *Proc Natl Acad Sci USA* 105:12271–6.
40. Wang, J., L. Xu, E. Wang, and S. Huang, 2010. The Potential Landscape of Genetic Circuits Imposes the Arrow of Time in Stem Cell Differentiation. *Biophys J* 99:29–39.
41. Waddington, C. H., 1957. The Strategy of the Genes: A Discussion of Some Aspects of Theoretical Biology. George Allen & Unwin.
42. Siegal-Gaskins, D., M. K. Mejia-Guerra, G. D. Smith, and E. Grotewold, 2011. Emergence of Switch-Like Behavior in a Large Family of Simple Biochemical Networks. *PLoS Comput Biol* 7:e1002039.
43. Graf, T., and M. Stadtfeld, 2008. Heterogeneity of embryonic and adult stem cells. *Cell stem cell* 3:480–3.
44. Mueller-Sieburg, C. E., R. H. Cho, M. Thoman, B. Adkins, and H. B. Sieburg, 2002. Deterministic regulation of hematopoietic stem cell self-renewal and differentiation. *Blood* 100:1302–1309.
45. Chang, H. H., M. Hemberg, M. Barahona, D. E. Ingber, and S. Huang, 2008. Transcriptome-wide noise controls lineage choice in mammalian progenitor cells. *Nature* 453:544–7.
46. Warren, P. B., and P. R. ten Wolde, 2005. Chemical models of genetic toggle switches. *J Phys Chem B* 109:6812–23.

47. Akashi, K., X. He, J. Chen, H. Iwasaki, C. Niu, B. Steenhard, J. Zhang, J. Haug, and L. Li, 2003. Transcriptional accessibility for genes of multiple tissues and hematopoietic lineages is hierarchically controlled during early hematopoiesis. *Blood* 101:383–389.
48. Narula, J., A. M. Smith, B. Gottgens, and O. A. Igoshin, 2010. Modeling reveals bistability and low-pass filtering in the network module determining blood stem cell fate. *PLoS Comput Biol* 6:e1000771.
49. Rieger, M. A., P. S. Hoppe, B. M. Smejkal, A. C. Eitelhuber, and T. Schroeder, 2009. Hematopoietic cytokines can instruct lineage choice. *Science* 325:217–8.
50. Heyworth, C., S. Pearson, G. May, and T. Enver, 2002. Transcription factor-mediated lineage switching reveals plasticity in primary committed progenitor cells. *The EMBO journal* 21:3770–81.
51. Kashiwagi, A., I. Urabe, K. Kaneko, and T. Yomo, 2006. Adaptive response of a gene network to environmental changes by fitness-induced attractor selection. *PloS one* 1:e49.
52. Morelli, M. J., S. Tanase-Nicola, R. J. Allen, and P. R. ten Wolde, 2008. Reaction coordinates for the flipping of genetic switches. *Biophys J* 94:3413–23.

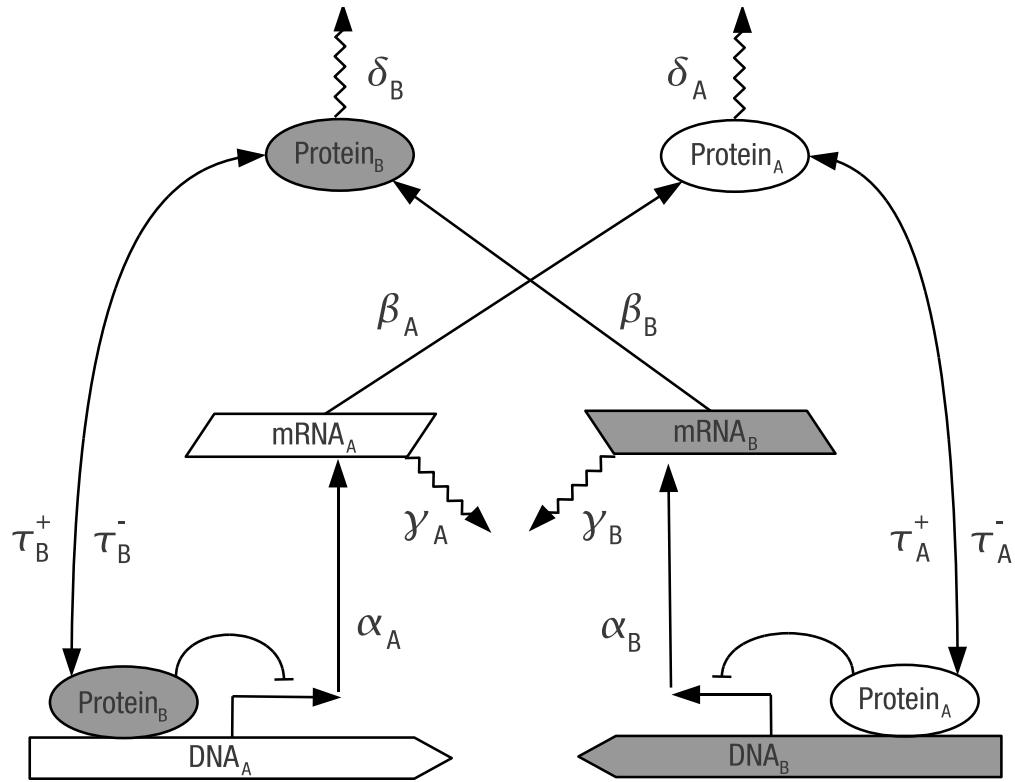


Figure 1: Scheme of the two-stage switch. Species associated with gene A are shown in white, species associated with B are shown in gray. Solid arrows indicate synthesis and binding, jagged arrows indicate degradation. mRNA_A is transcribed from DNA_A with rate α_A . It decays with rate γ_A and is translated into Protein_A with rate β_A . Protein_A decays with rate δ_A and can bind (unbind) DNA_B with rate τ_A^+ (τ_A^-). Protein-bound DNA leads to transcriptional arrest. The topology is symmetric with respect to the genes A and B, thus, the same reactions exist for B.

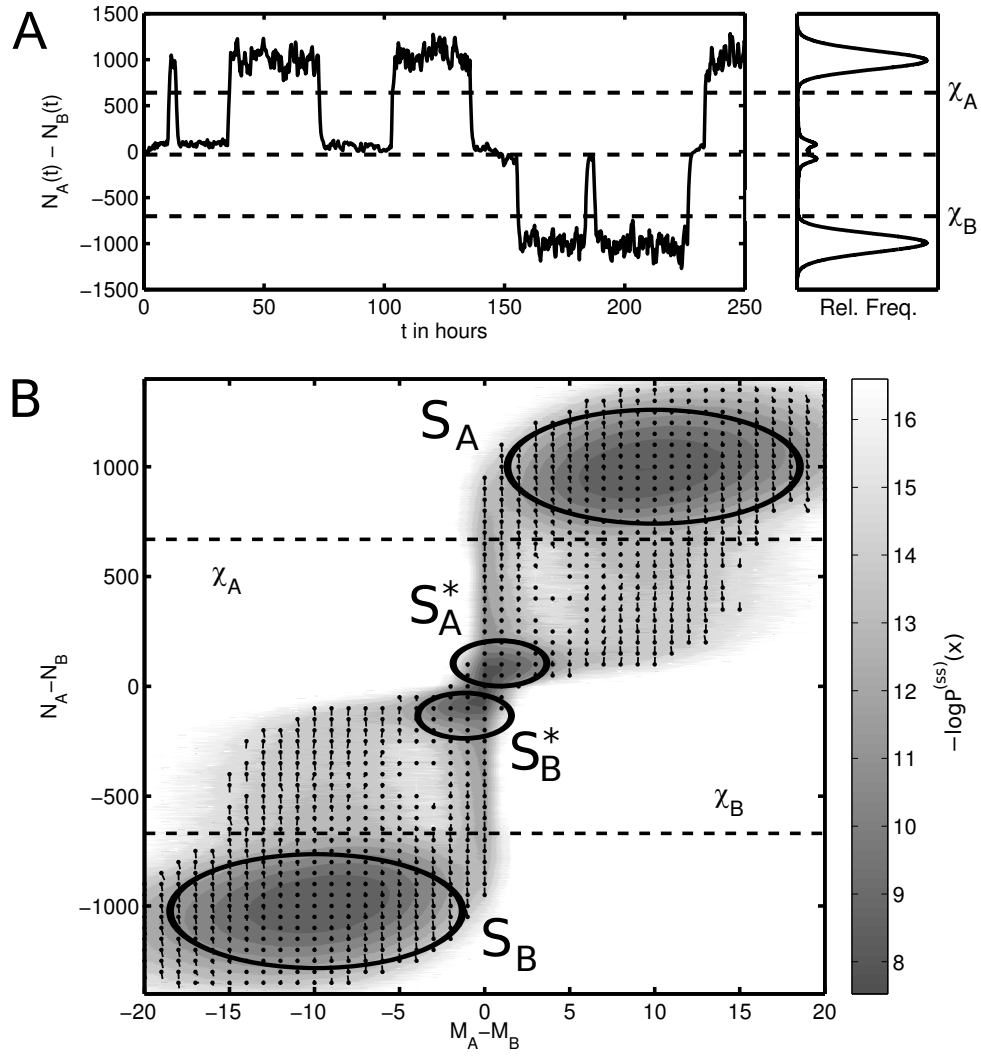


Figure 2: Dynamics and quasi-potential of the switch showing the different attractors of the system. (A) The timecourse of $N_A(t) - N_B(t)$ clearly shows the dominating attractors, which can be separated in state space via the thresholds χ_A and χ_B . Either A dominates (attractor S_A), or B dominates (attractor S_B), or the system is temporarily locked by two bound promoters with only marginal protein expression of A or B (attractors S_A^* and S_B^*). A histogram of $N_A(t) - N_B(t)$ is shown on the right. (B) The quasi-potential, defined as $U(x) = -\log P^{(ss)}(x)$, includes the mRNA dimension of the system. It shows the four possible attractors as basins in a probability landscape. S_A and S_B are visible as basins at the lower left and upper right corners, whereas S_A^* and S_B^* are located around the origin ($N_A - N_B = M_A - M_B = 0$) of the landscape. Additionally, the outflux $F(x)$ acting on the system at the state x in state space are indicated as lines (circles correspond to the origin of the vector). Note that the outflux is different from concept of deterministic field lines. These vectors show that there are different paths for entering and leaving the dominating attractors. Parameters for the simulation are given in Table S1.

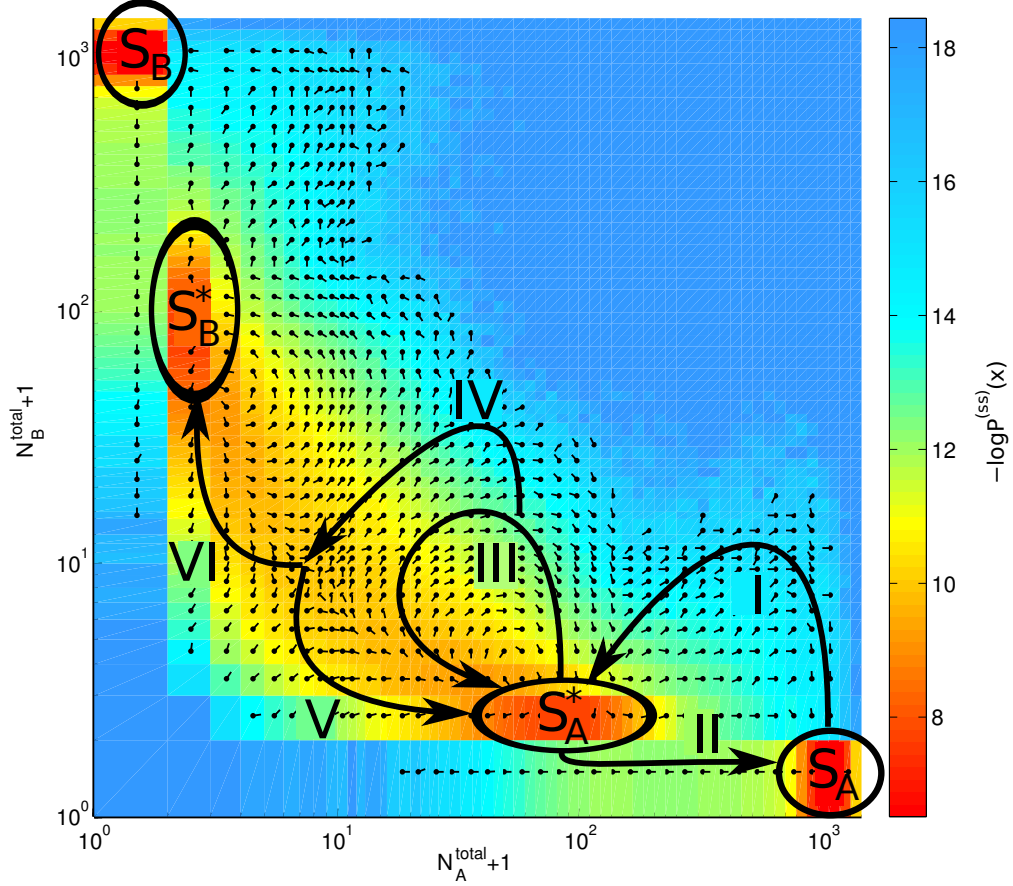


Figure 3: Quasi-potential of the system projected onto the N_A^{total} and N_B^{total} dimensions. Note that both axis are on logarithmic scale and are shifted by 1 in order to include $N_A^{\text{total}} = 0$ and $N_B^{\text{total}} = 0$. Therefore the lowest row in the plot corresponds to the case $N_B^{\text{total}} = 0$. The quasi-potential $U(x) = -\log \mathcal{P}^{(ss)}(x)$ is color coded where red areas reflect minima of the landscape. Visible are four minima corresponding to S_A (lower right), S_B (upper left), S_A^* (lower middle) and S_B^* (middle left). The vectors of the outflux at each point in state space are drawn as lines (circles correspond the the origin of the vector). Note that the outflux is different from concept of deterministic field lines. In contrast to Fig. 2 the vectors are normalized and therefore show only the direction, not the magnitude of the field. Bold arrows reflect typical trajectories (I-VI) of the system. For a discussion, see the main text.

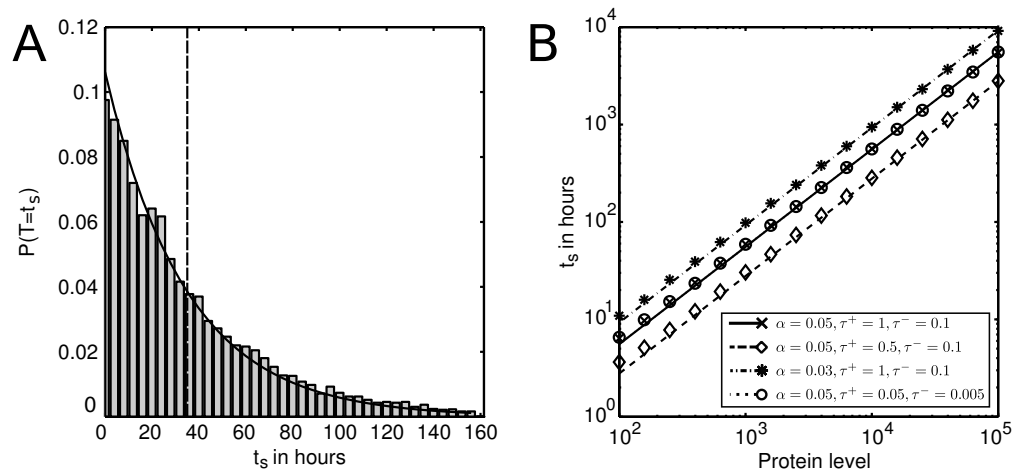


Figure 4: Residence time t_s in the two-stage toggle switch. (A) The distribution for t_s obtained by stochastic simulation is in good agreement with the geometric distribution derived from our mean-field approximation. The mean of the distribution is indicated by a dashed line. The protein decay rate was set to $\delta = 8 \cdot 10^{-4} s^{-1}$. (B) Mean residence time t_s versus mean protein level \bar{N} derived from stochastic simulation (symbols) and our analytical approximation (lines) for four different parameter settings. Note that the analytical approximations as well as the simulation results of the first and fourth parameter set coincide. The exponent in the relation $t_s \propto (\bar{N}_A)^\nu$ is $\nu = 1$, in accordance with equation 14.

Supporting Material

Stability and multi-attractor dynamics of a toggle switch based on a two-stage model of stochastic gene expression

Michael Strasser

Institute for Bioinformatics and Systems Biology,
Helmholtz Zentrum München
German Research Center for Environmental Health, Germany

Fabian J. Theis

Institute for Bioinformatics and Systems Biology,
Helmholtz Zentrum München
German Research Center for Environmental Health, Germany
and
Institute for Mathematical Sciences,
Technische Universität München
Garching, Germany

Carsten Marr^{1 2}

Institute for Bioinformatics and Systems Biology,
Helmholtz Zentrum München
German Research Center for Environmental Health, Germany

February 19, 2022

¹Corresponding author. Address: Institute for Bioinformatics and Systems Biology, Helmholtz Zentrum München, Ingolstaedter Landstrasse 1, 85764 Neuherberg, Germany, Tel.: +49 (0)89 3187 3642, Fax: +49 (0)89 3187 3585, Email: carsten.marr@helmholtz-muenchen.de

²Present address: Centre for Systems Biology at Edinburgh, University of Edinburgh, Edinburgh EH9 3JD, UK

1 Steady state solution of the deterministic two-stage toggle switch

Using symmetric parameters $\alpha = \alpha_A = \alpha_B$, $\beta = \beta_A = \beta_B$, $\gamma = \gamma_A = \gamma_B$, $\delta = \delta_A = \delta_B$, $\tau^+ = \tau_A^+ = \tau_B^+$ and $\tau^- = \tau_A^- = \tau_B^-$ results in two following steady state solutions of equations (7), (8) and (9) in the main text:

$$m_A^{(1)} = m_B^{(1)} = -\frac{\delta\tau^-}{2\beta\tau^+} (1 - \eta) \quad (\text{S1})$$

$$n_A^{(1)} = n_B^{(1)} = -\frac{\tau^-}{2\tau^+} (1 - \eta) \quad (\text{S2})$$

$$d_A^{(1)} = d_B^{(1)} = \frac{2}{1 + \eta} \quad (\text{S3})$$

$$m_A^{(2)} = m_B^{(2)} = -\frac{\delta\tau^-}{2\beta\tau^+} (1 + \eta) \quad (\text{S4})$$

$$n_A^{(2)} = n_B^{(2)} = -\frac{\tau^-}{2\tau^+} (1 + \eta) \quad (\text{S5})$$

$$d_A^{(2)} = d_B^{(2)} = \frac{2}{1 - \eta} \quad (\text{S6})$$

with $\eta = \sqrt{\frac{4\alpha\beta\tau^+}{\gamma\delta\tau^-} + 1}$. The first solution is positive, the second is negative (given all parameters are positive). Only the positive solution is of interest in biological systems. The monostability of this system is due to the monomeric protein binding. As soon as dimeric binding is introduced, the system becomes multistable, similar to the existing one-stage deterministic models (1-3).

Note that for small τ^+ equations (S1) and (S2) reduce to the steady state solution of a simple two stage expression model

$$\begin{aligned} n_A^{(1)} = n_B^{(1)} &= \frac{\alpha\beta}{\gamma\delta} \\ m_A^{(1)} = m_B^{(1)} &= \frac{\alpha}{\gamma}, \end{aligned}$$

because

$$\eta \approx 1 + \frac{2\alpha\beta\tau^+}{\gamma\delta\tau^-}$$

for small τ^+ through the Taylor approximation

$$(1 + x)^n \approx 1 + nx \text{ for } |x| \ll 1.$$

This is expected since setting τ^+ to 0 removes the interaction between both players, which will then evolve independently according to a two-stage expression model.

For decreasing τ^- the solution of the system approaches the origin

$$\begin{aligned} n_A^{(1)} = n_B^{(1)} &= 0 \\ m_A^{(1)} = m_B^{(1)} &= 0 \end{aligned}$$

because $\eta \approx \frac{\text{const}}{\sqrt{\tau^-}}$ and therefore the right hand sides of equations (S1) and (S2) reduce to $\text{const} \cdot \frac{\tau^-}{\sqrt{\tau^-}}$. For decreasing τ^- this term will approach 0. Hence, if proteins never unbind the promoter, the system will be locked forever yielding 0 protein and mRNA levels in steady state.

We now assess the stability of the positive solution (S1) - (S3) using standard linear stability analysis. To reduce the complexity of our system for the stability analysis, we apply a quasi steady state approximation to the DNA binding/dissociation process ($\dot{d}_A = \dot{d}_B = 0$), reducing the dimensionality of our system to four equations:

$$\begin{aligned}\frac{d}{dt}m_A &= \alpha\psi(n_B) - \gamma m_A \\ \frac{d}{dt}m_B &= \alpha\psi(n_A) - \gamma m_B \\ \frac{d}{dt}n_A &= \beta m_A - \delta n_A + \tau^-(1 - \psi(n_A)) - \tau^+\psi(n_A)n_A \\ \frac{d}{dt}n_B &= \beta m_B - \delta n_B + \tau^-(1 - \psi(n_B)) - \tau^+\psi(n_B)n_B,\end{aligned}$$

with $\psi(x) = \frac{\tau^-}{\tau^- + x \cdot \tau^+}$. The reduced system has the positive steady state solution

$$m_A^{(ss)} = m_B^{(ss)} = -\frac{\delta\tau^-}{2\beta\tau^+} (1 - \eta) \quad (\text{S7})$$

$$n_A^{(ss)} = n_B^{(ss)} = -\frac{\tau^-}{2\tau^+} (1 - \eta) \quad (\text{S8})$$

with $\eta = \sqrt{\frac{4\alpha\beta\tau^+}{\gamma\delta\tau^-} + 1}$. Notice that this is the same as the solution for mRNA and protein of the full system (Eq. (S1) and Eq. (S2)). We calculate the Jacobian matrix of the reduced system as

$$J = \begin{pmatrix} -\gamma & 0 & 0 & \frac{\alpha\tau^+}{\tau^-} \cdot \psi^2(n_B) \\ 0 & -\gamma & \frac{\alpha\tau^+}{\tau^-} \cdot \psi^2(n_A) & 0 \\ \beta & 0 & -\delta + \tau^+\psi^2(n_A)[1 + \tau^+n_A - \psi^{-1}(n_A)] & 0 \\ 0 & \beta & 0 & -\delta + \tau^+\psi^2(n_B)[1 + \tau^+n_B - \psi^{-1}(n_B)] \end{pmatrix}.$$

We evaluate the Jacobian at the steady state solution of the reduced system (Eq. (S7)-(S8)) and use the Hurwitz criterion to verify that all its eigenvalues have negative real part. We conclude that the system has one stable positive fixed point but we cannot analytically exclude the existence of limit cycles. However, inspection of the system's phase portrait (see Fig. S4) indicates that no limit cycles exist.

2 Master equation

The stochastic model of the two-stage switch is completely defined by the master equation. We define $\mathcal{P}_{ij}(M_A, M_B, N_A, N_B, t)$ as the probability at time t to have M_A copies of mRNA_A, M_B copies of mRNA_B, N_A copies of Protein_A, N_B copies of Protein_B, and the corresponding promoter configuration ij where 0 (1) means an unbound (bound) promoter. This results in the following master equation that is split up into four coupled equations, corresponding to the four promoter states:

$$\begin{aligned}
\frac{d}{dt}\mathcal{P}_{00}(M_A, M_B, N_A, N_B, t) &= \tau_A^- E_{N_A}^- \mathcal{P}_{01}(M_A, M_B, N_A, N_B, t) + \tau_B^- E_{N_B}^- \mathcal{P}_{10}(M_A, M_B, N_A, N_B, t) \\
&\quad + [-\tau_B^+ N_B - \tau_A^+ N_A + \alpha_A (E_{M_A}^- - 1) + \alpha_B (E_{M_B}^- - 1) + \gamma_A (E_{M_A}^+ - 1) \cdot M_A + \gamma_B (E_{M_B}^+ - 1) \cdot M_B \\
&\quad + \beta_A (E_{N_A}^- - 1) \cdot M_A + \beta_B (E_{N_B}^- - 1) \cdot M_B + \delta_A (E_{N_A}^+ - 1) \cdot N_A + \delta_B (E_{N_B}^+ - 1) \cdot N_B] \\
&\quad \cdot \mathcal{P}_{00}(M_A, M_B, N_A, N_B, t) \\
\frac{d}{dt}\mathcal{P}_{11}(M_A, M_B, N_A, N_B, t) &= \tau_A^+ E_{N_A}^+ N_A \mathcal{P}_{10}(M_A, M_B, N_A, N_B, t) + \tau_B^+ E_{N_B}^+ N_B \mathcal{P}_{01}(M_A, M_B, N_A, N_B, t) \\
&\quad + [-\tau_A^- - \tau_B^- + \gamma_A (E_{M_A}^+ - 1) \cdot M_A + \gamma_B (E_{M_B}^+ - 1) \cdot M_B \\
&\quad + \beta_A (E_{N_A}^- - 1) \cdot M_A + \beta_B (E_{N_B}^- - 1) \cdot M_B + \delta_A (E_{N_A}^+ - 1) \cdot N_A + \delta_B (E_{N_B}^+ - 1) \cdot N_B] \\
&\quad \cdot \mathcal{P}_{11}(M_A, M_B, N_A, N_B, t) \\
\frac{d}{dt}\mathcal{P}_{10}(M_A, M_B, N_A, N_B, t) &= \tau_A^- E_{N_A}^- \mathcal{P}_{11}(M_A, M_B, N_A, N_B, t) + \tau_B^+ E_{N_B}^+ N_B \mathcal{P}_{00}(M_A, M_B, N_A, N_B, t) \\
&\quad + [-\tau_B^- - \tau_A^+ N_A + \alpha_B (E_{M_B}^- - 1) + \gamma_A (E_{M_A}^+ - 1) \cdot M_A + \gamma_B (E_{M_B}^+ - 1) \cdot M_B \\
&\quad + \beta_A (E_{N_A}^- - 1) \cdot M_A + \beta_B (E_{N_B}^- - 1) \cdot M_B + \delta_A (E_{N_A}^+ - 1) \cdot N_A + \delta_B (E_{N_B}^+ - 1) \cdot N_B] \\
&\quad \cdot \mathcal{P}_{10}(M_A, M_B, N_A, N_B, t) \\
\frac{d}{dt}\mathcal{P}_{01}(M_A, M_B, N_A, N_B, t) &= \tau_A^+ E_{N_A}^+ N_A \mathcal{P}_{00}(M_A, M_B, N_A, N_B, t) + \tau_B^- E_{N_B}^- \mathcal{P}_{11}(M_A, M_B, N_A, N_B, t) \\
&\quad + [-\tau_B^+ N_B - \tau_A^- + \alpha_A (E_{M_A}^- - 1) + \gamma_A (E_{M_A}^+ - 1) \cdot M_A + \gamma_B (E_{M_B}^+ - 1) \cdot M_B \\
&\quad + \beta_A (E_{N_A}^- - 1) \cdot M_A + \beta_B (E_{N_B}^- - 1) \cdot M_B + \delta_A (E_{N_A}^+ - 1) \cdot N_A + \delta_B (E_{N_B}^+ - 1) \cdot N_B] \\
&\quad \cdot \mathcal{P}_{01}(M_A, M_B, N_A, N_B, t) .
\end{aligned}$$

The shift operators E_x^+ and E_x^- increase or decrease the function argument x by one, $E_x^\pm f(x) = f(x \pm 1)$. To our knowledge no results have yet been published on the solution of stochastic two-stage switches.

Reaction	Parameter value
Transcription α	$0.05 s^{-1}$
Translation β	$0.05 s^{-1} \text{mRNA}^{-1}$
mRNA degradation γ	$0.005 s^{-1}$
Protein degradation δ	$5 \cdot 10^{-3}$ to $5 \cdot 10^{-6} s^{-1}$
DNA binding τ^+	$1 s^{-1} \text{Protein}^{-1}$
DNA dissociation τ^-	$0.1 s^{-1}$

Table S1: Parameters of the switch model used throughout this work. Protein degradation is chosen according to the desired protein level n . If not mentioned otherwise, all simulations and plots are based on this set of parameters.

3 Rates

First we derive upper boundaries for the transcription and translation rates. Transcription of DNA into mRNA is accomplished by the RNA-polymerase. One polymerase can process about 10-20 nucleotides (nt) per second in eucaryotes (4–6). As described by Alberts et al. (4) the newly elongated RNA fragment is immediately released from the DNA, which enables other polymerases to follow up even before the first mRNA has been completed. The distance d between polymerases is estimated to be around 100 nt (7). The rate of transcription is independent of the sequence length l , since the longer the gene, the more polymerases can process it in parallel. Altogether we find the maximal transcription rate α by dividing the speed of transcription v with the sequence length l , multiplied with the number of transcribing polymerases,

$$\alpha = \frac{v}{l} \cdot \frac{n}{d} \approx \frac{10 \text{ nt/s}}{l} \cdot \frac{l}{100 \text{ nt}} = 0.1s^{-1}$$

required that enough polymerases and nucleotides are present.

The maximal translation rate can be inferred in a similar way: Ribosomes, large complexes of proteins and rRNAs that translate mRNA into polypeptides, proceed with a speed v of 2 codons (= 6 nt = 2 amino acids) per second in eucaryotes (4). One mRNA can be processed by many ribosomes (polyribosomes) at the same time (4). The average space between two ribosomes is 80 nt or ≈ 27 amino acids (AA). (4). Therefore the overall translation rate for an mRNA of length n is

$$\beta \approx \frac{2\text{AA/s}}{l} \frac{l}{27\text{AA}} = 0.074s^{-1},$$

again independent of the mRNA length l . This corresponds to the maximally possible translation rate. The actual rate will be smaller when not enough ribosomes or other involved molecules (tRNA, amino acids) are present. We estimate the minimal translation time as $1/0.074s^{-1} = 13.5s$, which is in good agreement with literature, where the time needed for one translation is said to be between 20 seconds and several minutes (4). Notably, these transcription and translation rates only provide rough estimates of the relevant timescale. Throughout the manuscript, we use a transcription and translation rate of $\alpha = \beta = 0.05 s^{-1}$, corresponding to an average time of 20 seconds per product, which seems to be reasonable in the context of the above considerations. The fact that both rates are equal is not expected to have influences on the results.

Interactions between proteins and DNA are mediated by specific regions of the proteins, called DNA-binding domains, which on the one hand can recognize specific DNA sequences and on the other hand maintain the interaction between DNA and protein. Zinc Fingers, Leucine Zippers or Helix-Turn-Helix motifs are prominent examples of DNA binding domains (4). The binding between DNA and protein is maintained by hydrogen bonds, ionic bonds, and hydrophobic interactions. Single interactions are weak, but as many bonds are formed, the binding between DNA and protein becomes stronger. The binding rates are very fast compared to transcription and translation processes and according to Alon (8) in the range of $1s^{-1}\text{Protein}^{-1}$ in *Eschericia coli*. The unbinding rate depends on the strength of the interaction and is assumed to be 10 times smaller ($0.1s^{-1}$) in our model, leading to strong binding of the protein to the DNA. All reaction rates of the models used in this work are summarized in Table S1.

As we showed above, the transcription and translation rates have upper bounds. The only way for a cellular system to further increase the abundance of proteins is to modulate the degradation rates of mRNA or proteins, giving longer lifetimes to mRNA and proteins. Thus, during this work we manipulate the degradations rates to adjust the system’s protein level to a desired steady state. Notably, following the report of Warren et al. (9), mRNA levels are set to 10 by adjusting the decay rate.

4 Attractor boundaries

In this section we assume symmetric parameters for both players ($\alpha = \alpha_A = \alpha_B, \dots$) for simplicity.

4.1 S_A and S_B

We approximate the protein number distribution in the attractors S_A and S_B using results from Thattai and van Oudenaarden (10), who showed that for a simple two-state expression model, the mean and variance of protein numbers obey

$$\bar{N} = \frac{\alpha\beta}{\gamma\delta} \quad \text{and} \quad \sigma^2 = \frac{\beta^2\alpha}{\gamma^2\delta + \delta^2\gamma},$$

respectively. Thereby, we assume that in the dominating attractors, the presence of the antagonist can be neglected due to its marginal transcription. We define the boundary χ_x of attractor S_x using a normal approximation of the dominating protein's distribution as

$$\chi_x = \bar{N}_x - Z_q \cdot \sigma_x, \quad (\text{S9})$$

where Z_q is the $q\%$ quantile of the standard normal distribution of the protein number with mean $\langle n \rangle_x$ and standard deviation σ_x . Using $q = 0.1$ throughout our study assures that 99.9% percent probability mass of the distribution lies beyond the lower boundary. Therefore we are certain to capture all relevant protein numbers belonging to S_A and S_B . Using these boundaries, we can define the attractors S_A , S_B , and S_0 accordingly:

$$\begin{aligned} S_A &= \{s \in S | N_A > \chi_A \wedge N_B < \chi_B\} \\ S_B &= \{s \in S | N_A < \chi_A \wedge N_B > \chi_B\} \\ S_0 &= \{s \in S | N_A < \chi_A \wedge N_B < \chi_B\}. \end{aligned}$$

4.2 S_A^* and S_B^*

In the S_A^*/S_B^* states, one protein of the 'repressed' species is present, partially blocking the promoter of the dominating player. Therefore the dominating player is not synthesized with full rate and its protein level will be smaller:

The promoter of the dominating player A is free only $100 \cdot \frac{\tau^-}{\tau^+ + \tau^-} \%$ of the time. Therefore the average number of mRNA_A in this attractor is $m = \frac{\tau^-}{\tau^+ + \tau^-} \cdot \frac{\alpha}{\gamma}$ (compared to $\frac{\alpha}{\gamma}$ at full synthesis). Consequently the average number of Protein_A in the state S_A^* will be

$$\bar{N}_A = m \cdot \frac{\beta}{\delta} = \frac{\tau^-}{\tau^- + \tau^+} \cdot \frac{\alpha\beta}{\gamma\delta}. \quad (\text{S10})$$

Based on this finding one can construct boundaries in a similar way to the S_A/S_B attractors.

5 Implications for Differentiation

In the following, we assume that only if one player dominates the other one for a sufficiently long time t_d , downstream genes necessary for the decision process are activated (e.g. leading to chromatin remodeling),

and the cell differentiates. We are thus interested in the probability that the residence time T in a dominating attractor is longer than t_d :

$$\omega = P(T \geq t_d) .$$

This can easily be evaluated using the previous results on the residence time. Each time the switch flips, the system has the chance to settle in a sufficiently long residence time. What is the probability that after switching m times the residence time is greater than t_d ? We therefore define a random variable M representing the number of switching events until the residence time is greater than t_d and find that it follows a geometric distribution with parameter ω :

$$P(M = m) = \omega(1 - \omega)^{m-1} .$$

This distribution tells us how likely it is to find a cell differentiated after m switching events. It is non-trivial to directly relate m to the time until differentiation (further denoted by the random variable T_p) since this time is composed of the actual realizations of the residence time and the time the system spends in the intermediate attractors. As no analytic expression of the time in the intermediate attractors S_A^* and S_B^* is available, we do not take into account the time spent in S_A^* and S_B^* but only the residence time of the system in S_A and S_B .

Now the time until differentiation only depends on the $m - 1$ independent realizations of the residence time (see Fig. S1A):

$$T_p = \sum_i^{m-1} T_i .$$

The system flips the attractors $m - 1$ times and resides here for a time given by T_i until it stays in one dominating attractor for a time longer than t_d . T_p is a sum of random variables T_i but also the number of summands varies according to the random variable M .

Another obstacle is the fact that the T_i are not exact geometric random variables, but truncated above t_d . For simplicity we do not make this distinction here. This is justified for small ω , because ω determines the fraction of probability mass that is truncated.

It can be shown that the sum Z of n geometric random variables T_i with common parameter p follows a negative binomial distribution:

$$Z = \sum_{i=1}^n T_i \sim NB(n, p)$$

$$P(Z = z) = \binom{z + n - 1}{z} (1 - p)^n p^z .$$

Since in our case n is drawn from a distribution itself, we have to consider the compound distribution (11) of M and Z to ultimately obtain the probability density function for T_p , which is a combination of how many switching events take place (represented by M) and the actual time the system spends in the dominating attractors (represented by the T_i):

$$\begin{aligned}
P(T_p = t) &= \sum_{m=1}^{\infty} P(M = m)P(T_p = t|M = m) \\
&= \sum_{m=1}^{\infty} \omega(1 - \omega)^{m-1} \binom{t + (m - 1) - 1}{t} (1 - p)^{m-1} p^t \\
&= \begin{cases} -(1 - p)^t p [1 + p(-1 + \omega)]^{-1-t} (-1 + \omega) \omega & t > 0 \\ \frac{\omega}{1 + p(-1 + \omega)} & t = 0 \end{cases} .
\end{aligned}$$

(A special case has to be considered for $m = 1$, where the system immediately starts differentiating. Here one has to define $P(T_p = 0|M = 1) = \omega$ and $P(T_p > 0|M = 1) = 0$, since the negative binomial distribution $NB(n, p)$ is meaningless for $n = 0$).

Fig. S1 B shows the distribution of T_p for a mean residence time $t_s = 1h$ and a threshold of $t_d = 5h$, meaning that the system has to reside for more than $5h$ in the same attractor to promote differentiation. Immediate differentiation is most probable ($t = 0$) and the probability for higher differentiation times decreases quickly. Therefore the majority of cells will differentiate rapidly and only few cells will need longer time to differentiate. This is somewhat counterintuitive, since one would expect that it takes a long time until a sufficiently large residence time $> t_d$ has been accomplished to promote differentiation (since longer residence times are less likely than shorter ones). However, due to the "odd" nature of the geometric distribution – where the probability for success is always the highest on the first try – the system has the highest chance to reach a sufficiently long residence time on the first try (reflected by the random variable M). Even if the system has to change attractors more often, the differentiation time will be short since the residence time in each attractor is most likely very small (since it is itself a geometric random variable), contributing only little to the overall differentiation time.

References

1. Roeder, I., and I. Glauche, 2006. Towards an understanding of lineage specification in hematopoietic stem cells: a mathematical model for the interaction of transcription factors GATA-1 and PU.1. *J Theor Biol* 241:852–865.
2. Huang, S., Y.-P. Guo, G. May, and T. Enver, 2007. Bifurcation dynamics in lineage-commitment in bipotent progenitor cells. *Dev Biol* 305:695–713.
3. Chickarmane, V., T. Enver, and C. Peterson, 2009. Computational Modeling of the Hematopoietic Erythroid-Myeloid Switch Reveals Insights into Cooperativity, Priming, and Irreversibility. *PLoS Comput Biol* 5:e1000268.
4. Alberts, B., A. Johnson, J. Lewis, M. Raff, K. Roberts, and P. Walter, 2002. Molecular biology of the cell. Garland Science.
5. Dahlberg, M. E., and S. J. Benkovic, 1991. Kinetic mechanism of DNA polymerase I (Klenow fragment): identification of a second conformational change and evaluation of the internal equilibrium constant. *Biochemistry* 30:4835–4843.

6. Singh, K., A. Srivastava, S. S. Patel, and M. J. Modak, 2007. Participation of the fingers subdomain of Escherichia coli DNA polymerase I in the strand displacement synthesis of DNA. *J Biol Chem* 282:10594–10604.
7. Kennell, D., and H. Riezman, 1977. Transcription and translation initiation frequencies of the Escherichia coli lac operon. *J Mol Biol* 114:1–21.
8. Alon, U., 2007. An introduction to systems biology: design principles of biological circuits. CRC Press.
9. Warren, L., D. Bryder, I. L. Weissman, and S. R. Quake, 2006. Transcription factor profiling in individual hematopoietic progenitors by digital RT-PCR. *Proc Natl Acad Sci USA* 103:17807–12.
10. Thattai, M., and A. van Oudenaarden, 2001. Intrinsic noise in gene regulatory networks. *Proc Natl Acad Sci USA* 98:8614–9.
11. Bailey, N. T. J., 1990. The Elements of Stochastic Processes with Applications to the Natural Sciences. Wiley-Interscience.
12. Hensold, J. O., C. a. Stratton, D. Barth, and D. L. Galson, 1996. Expression of the transcription factor, Spi-1 (PU.1), in differentiating murine erythroleukemia cells is regulated post-transcriptionally. *The Journal of biological chemistry* 271:3385–91.
13. Schwanhäusser, B., D. Busse, N. Li, G. Dittmar, J. Schuchhardt, J. Wolf, W. Chen, and M. Selbach, 2011. Global quantification of mammalian gene expression control. *Nature* 473:337–42.

6 Supplementary Figures

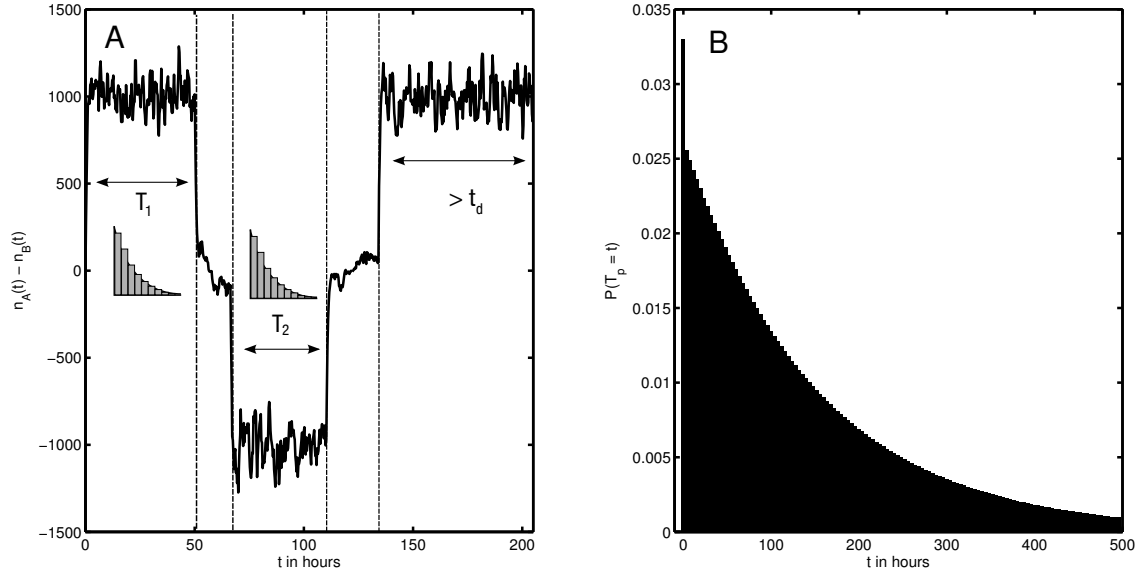


Figure S1: A: Scheme of the differentiation mechanism. The system changes the dominating attractor twice before it settles into S_A for a time greater than t_d , which induces differentiation. The residence times in S_A and S_B follow a (truncated) geometric distribution. The overall time until differentiation is therefore (neglecting the intermediate attractors) the sum of these geometric random variables. B: Distribution of the differentiation time T_p for a residence time of $1h$ and $t_d = 5h$. Small differentiation times are more probable than higher bigger differentiation times. Note the strong peak at $t = 0$ indicating that it is most probable for a cell to differentiate immediately .

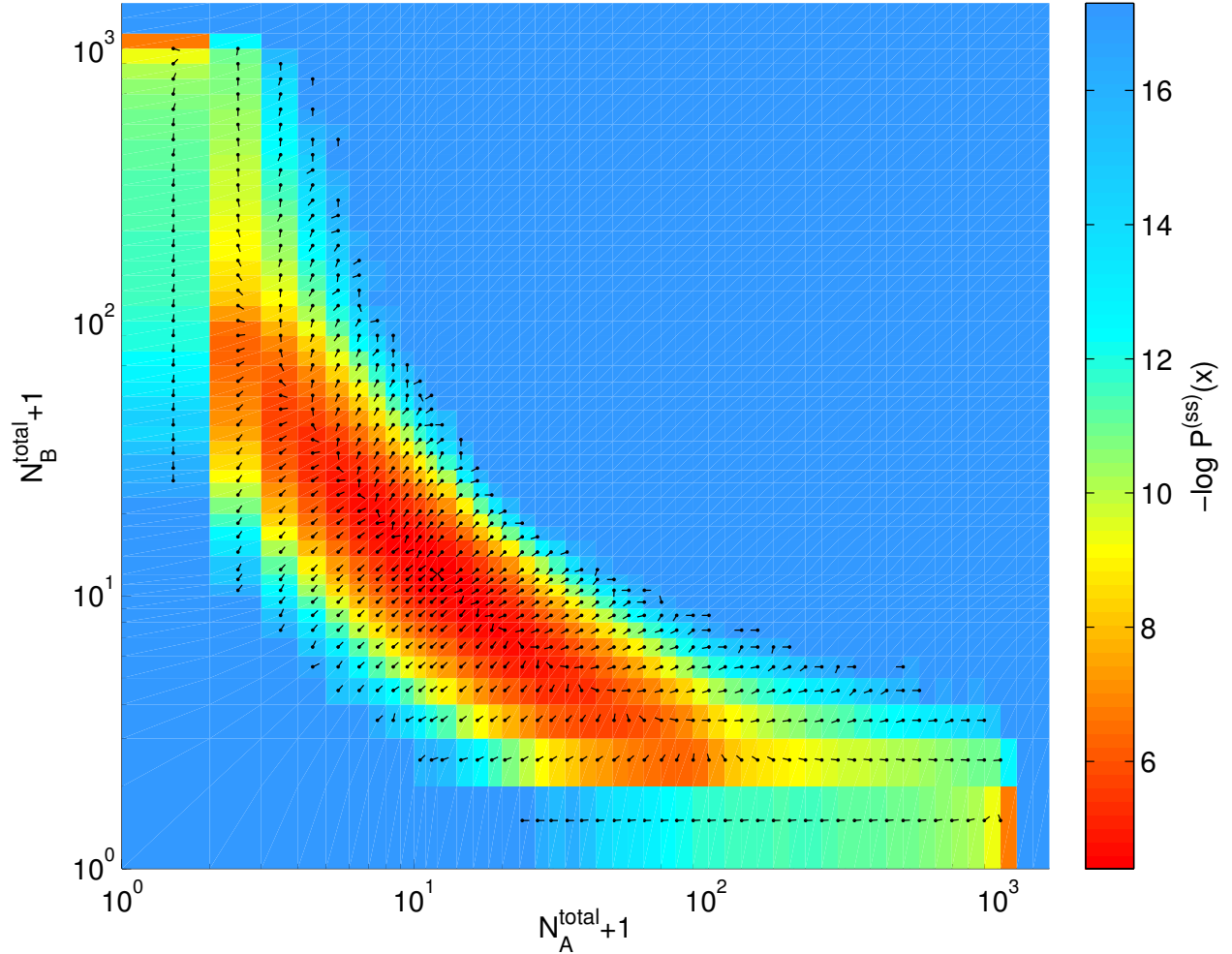


Figure S2: Quasi-potential of a toggle switch based on a one-stage expression model projected onto the N_A^{total} and N_B^{total} dimensions. Notice that both axis are on logarithmic scale and are shifted by 1 in order to include $N_A^{\text{total}} = 0$ and $N_B^{\text{total}} = 0$. Therefore the lowest row in the plot corresponds to the case $N_B^{\text{total}} = 0$. The quasi-potential $U(x) = -\log \mathcal{P}^{(ss)}(x)$ is color coded where red areas reflect minima of the landscape. Contrary to the two-stage toggle switch model only three attractors are present. The vectors of the outflux at each point in state space are drawn as lines (circles correspond to the origin of the vector). Vectors are normalized and therefore show only the direction, not the magnitude of the field. Parameters were set in accordance to the two-stage switch: Protein synthesis $\alpha = 0.5 \text{ s}^{-1}$, Protein degradation $\gamma = 5 \cdot 10^{-4} \text{ s}^{-1}$, DNA binding $\tau^+ = 1 \text{ Protein}^{-1} \text{ s}^{-1}$, DNA dissociation $\tau^- = 0.1 \text{ s}^{-1}$.

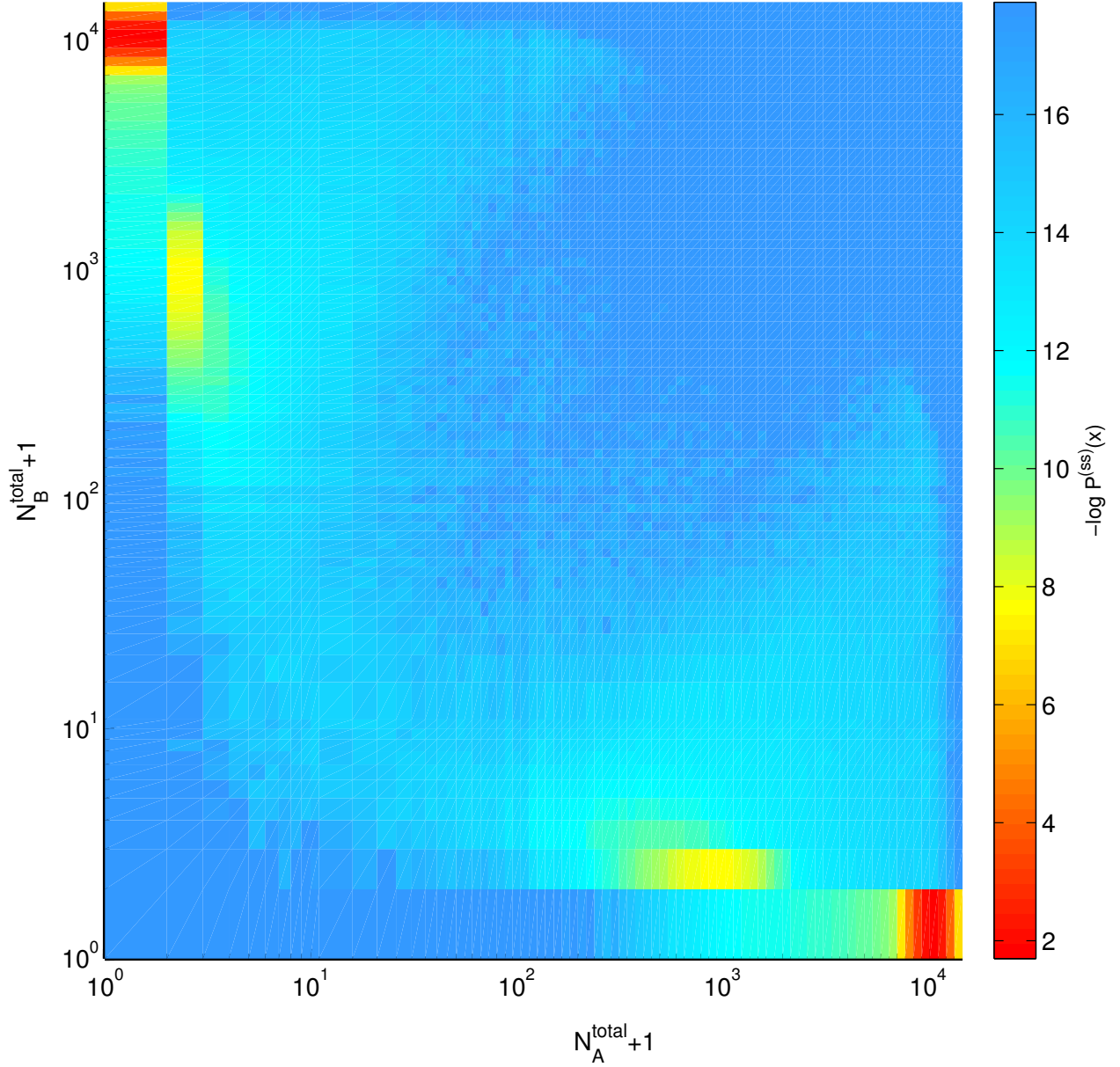


Figure S3: Quasi-potential of a two-stage toggle switch projected onto the N_A^{total} and N_B^{total} dimensions using a different parameter set: Motivated by Hensold et al. (12) we set the mRNA degradation rate to $\gamma = 3.6 \cdot 10^{-5} s^{-1}$ and adjust the transcription rate $\alpha = 3.6 \cdot 10^{-4} s^{-1}$ to obtain the desired 10 mRNAs per cell (9). Furthermore we set the protein degradation rate $\delta = 3.6 \cdot 10^{-6} s^{-1}$ as proteins are thought to be one order of magnitude more stable than mRNAs (13). The translation rate was set to $\beta = 0.0036 \text{ mRNA}^{-1} s^{-1}$ in accordance to (13). We observe the emergence of the same four attractors described in the main text and Fig. 3 therein.

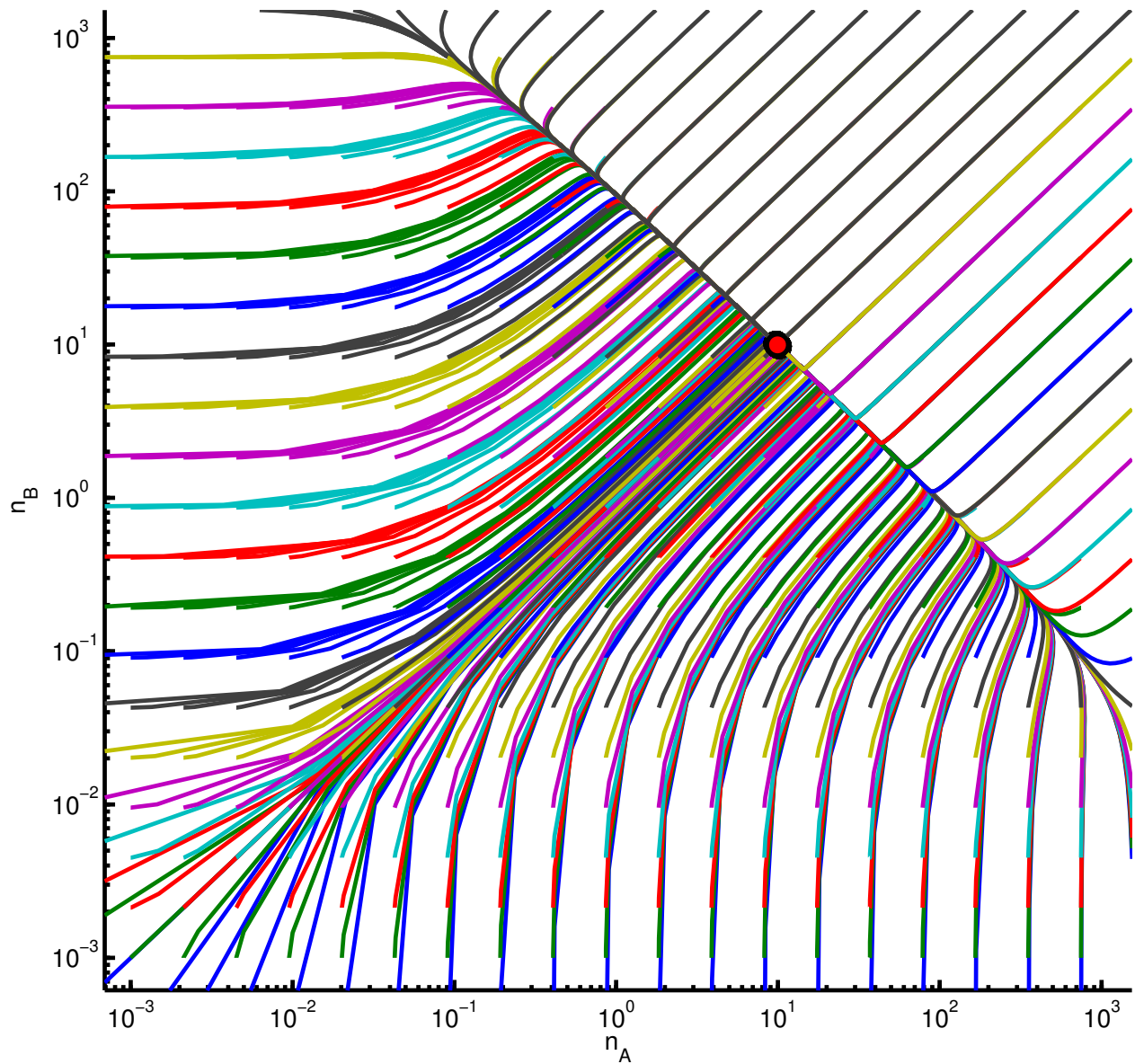


Figure S4: Phase portrait of the deterministic two-stage toggle switch model projected onto the N_A and N_B dimensions. The same parameters were used as in the probabilistic model of Fig. 2 and Fig. 3. The ODE was solved for different initial protein concentrations n_A, n_B and the mRNA concentrations were set to $m_A = 0.01 \cdot n_A$ and $m_B = 0.01 \cdot n_B$, resembling the fact that for the given parameters each mRNA will correspond to approximately 100 proteins. Trajectories are arbitrarily colored to improve readability. Note that trajectories can intersect as this is only a projection of the full system. Inspection of the phase portrait reveals the single steady state (red dot) as predicted by Eq. (S7) - (S8). No limit cycles are visible in the phase portrait.

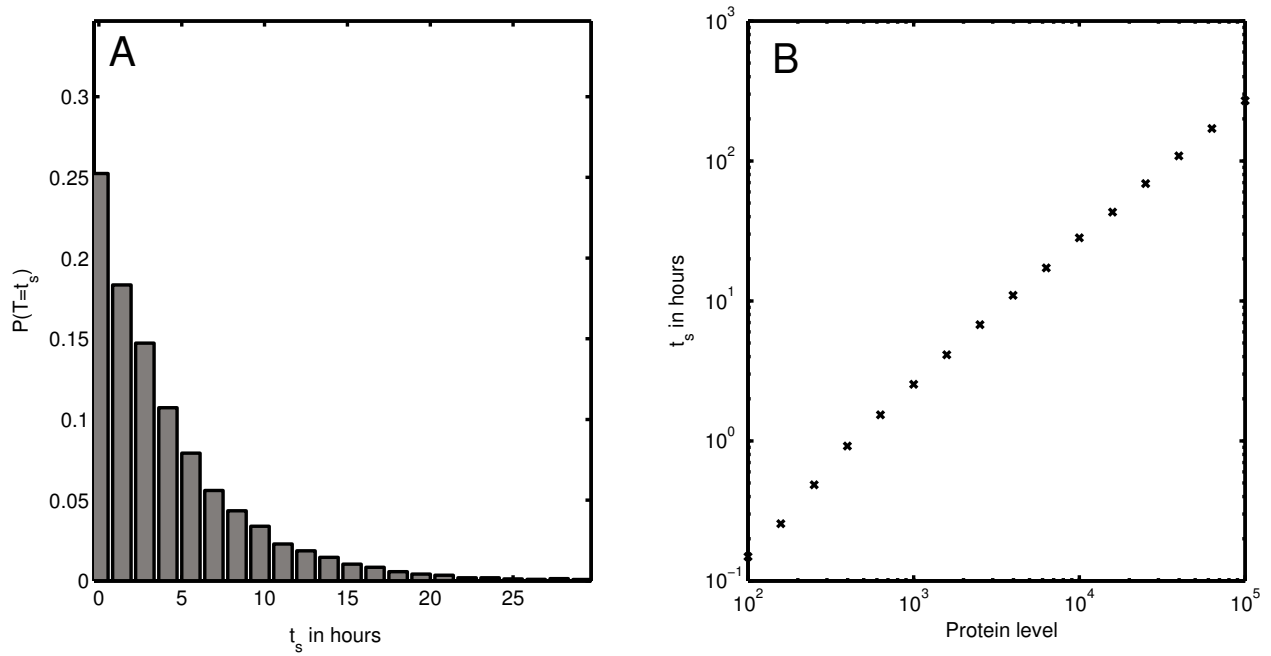


Figure S5: Residence time of the system in the intermediate attractors (S_A^* or S_B^*). (A) The histogram of the residence times in S_A^* obtained from stochastic simulation suggests that the residence time in the intermediate attractors follows a geometric distribution. (B) Similar to Fig. 4 one observes a linear scaling of the mean residence time and the protein abundance.